Journal of Archaeological Science 132 (2021) 105413

Contents lists available at ScienceDirect

Journal of Archaeological Science

journal homepage: www.elsevier.com/locate/jas

Deep learning artificial neural networks for non-destructive archaeological site dating

Kelsey M. Reese

Department of Anthropology, University of Notre Dame, Notre Dame, Indiana, 46556, United States

ARTICLE INFO

Keywords:
Machine learning
Deep learning
Artificial neural network
Dating
Demography
Mesa verde
US Southwest

ABSTRACT

This article introduces artificial neural networks as a computational tool to utilize legacy archaeological data for precisely and accurately estimating dates of residential site occupation. The implementation of this deep learning algorithm can provide high-resolution demographic reconstructions of a study area from non-collection, non-invasive, and non-destructive data collection methods that only record frequencies of artifact types on the contemporary ground surface. The utility of this deep learning algorithm is presented through an example from the central Mesa Verde region in the northern US Southwest. Results show a properly trained artificial neural network predicts annual residential occupation with an average 92.8% accuracy from AD 450–1300. An annual demographic reconstruction of the central Mesa Verde region using occupation predictions from the artificial neural network is also presented.

1. Introduction

Absolute dating of archaeological sites typically requires invasive and destructive scientific methods that yield results, at best, on a decadal timescale (Casanova et al., 2020; McIntosh and Catanzariti 2006; Roberts et al., 2015; Svetlik et al., 2019). The notable exception to this generalization is dendrochronology where dates are determined on an annual timescale (Douglas 1929), but consistent with other absolute dating techniques, dendrochronology is a type of destructive methodology that often requires invasive excavation projects to collect the necessary raw materials. However the time, resources, and permissions required to excavate and collect raw materials for absolute dating are not always attainable. Furthermore, archaeologists and native communities have long advocated for a move towards an archaeology of preservation and non-destructive research on cultural resources (Colwell-Chanthaphonh 2009; King and Lyneis 1978; Lipe 1974; Matero et al., 1998; Mills and Ferguson 1998).

Non-destructive methodologies for archaeological research have already proven useful for identifying subterranean structures with ground penetrating radar (Conyers 2018; Verdonck et al., 2020), finding cities beneath dense forest canopies using lidar (Chase et al., 2012; Inomata et al., 2020), and mapping changing river systems in ancient landscapes using satellite data (Orengo et al., 2019). Coupled with the growing use of these non-destructive techniques is the increased use of machine learning to reconstruct archaeological landscapes using computer vision (Caspari and Crespo 2019; Oonk and Spijker 2015), automating artifact identification in imagery collected by unmanned aerial vehicles (Orengo and Garcia-Molsosa 2019), and the implementation of predictive modeling to categorize artifacts within archaeological assemblages (Żabiński et al., 2020). The following analysis combines the move towards non-destructive archaeological research with the computational power of machine learning to provide a highly accurate, non-destructive tool for archaeological site dating.

This article introduces the use of artificial neural networks—trained using legacy archaeological data with absolute dating—to predict periods of archaeological site occupation using only surface artifact assemblages. The following sections will provide an overview of artificial neural networks, how they can be applied to archaeological datasets, and presents an annual demographic reconstruction in the northern US Southwest from AD 450–1300 to demonstrate the predictive power of this machine learning algorithm.

2. An overview of artificial neural networks

Artificial neural networks are a type of machine learning "inspired by the sophisticated functionality of human brains where hundreds of billions of interconnected neurons process information in parallel" (Wang 2003: 81). The synthetic analytical structure of artificial neural networks allows machines to recognize patterns in large and complex datasets by "distinguish[ing] patterns of interest from their background,

E-mail address: kreese1@nd.edu.

https://doi.org/10.1016/j.jas.2021.105413
Received 17 June 2020; Received in revised form 10 May 2021; Accepted 10 May 2021

and mak[ing] sound and reasonable decisions about the categories of the patterns" (Basu et al., 2010: 23). Artificial neural networks are constructed of three primary layers representing input information, output information, and the mathematical transformations that define the relationship between the two—the "hidden layer" (Krenker et al., 2011). Each layer consists of a series of nodes: in the input layer, each node represents a category of information; in the hidden layer, each node performs a mathematical transformation; and the output layer is most simplistically a single categorical node that represents the result (Krenker et al., 2011). The specific type of machine learning algorithm presented here is slightly more complex as it employs multiple nodes in the output layer, each representing a distinct outcome (Fig. 1), formally called a multi-label classification artificial neural network (Tsoumakas and Katakis 2007).

Artificial neural networks are trained on a dataset with known values for each node in the input layer and known values for each node in the output layer, but the neural network itself determines the values of each node within the hidden layer—making it a "deep learning" algorithm (LeCun et al., 2015)—where the computer can explore all options and relationships within a dataset without explicit direction from the researcher. The training process affords the model complete autonomy to identify which combinations of input nodes best predict corresponding output values. Each hidden node within the artificial neural network is used to define specific relationships within the provided dataset, and any number or combinations of inputs can be used by each hidden node as needed. Furthermore, the degree to which each input contributes information can vary among the hidden nodes, resulting in a model that can simultaneously consider input information wholly independently, and/or in any combination, to define divergent and complex relationships between the input and output values. Similarly, the multi-label classification artificial neural network predicts probabilities for each output node independently from all other nodes, allowing for the classification of information into multiple simultaneous categories—making this classification algorithm distinct from others, such as discriminant analyses, as the neural network does not calculate probabilities of outputs in relation or opposition to any other output. The model is ultimately trained through an iterative process that assigns weights to the input variables, sends the weighted values through the hidden nodes, and compares the predicted output values with the corresponding known output values. Differences between the predicted and known output values are then sent back through the model to inform changes in the weights assigned to each input variable before being sent through the model once again. This iterative process is repeated until the predicted values mimic the corresponding known values within a pre-defined error threshold. The mathematical processes occurring at each step of this process (and illustrated in Fig. 1) are briefly explained, below.

The artificial neural network trains itself through an iterative process that takes the information in the input nodes (x_i), and assigns weights (w_i) to each "synapse"—the line connecting each input node to each node in the hidden layer (Fig. 1, red lines). Fig. 1 highlights the independence each hidden node has when weighting individual input variables, as no weight (w_i) is dependent on any other. The sum of weights is calculated for each hidden node using Formula 1.

$$\phi\left(\sum_{i=1}^{m} w_i, x_i\right) \tag{1}$$

The summed values calculated within each hidden node are then passed through a logistic activation function (Formula 2) that determines the predicted value passed to the output nodes.

$$\phi(x) = \frac{1}{1+e^{-x}} \tag{2}$$

The resulting predicted values ($\hat{y}_i$) in the output nodes are directly compared to the corresponding known values (y_i), and the sum of squared errors (C) between predicted and known values is calculated (Formula 3).

$$C = \sum_{i=1}^{n} \frac{1}{2}(\hat{y}_i - y_i)^2 \tag{3}$$

If the sum of squared errors is greater than the pre-defined error

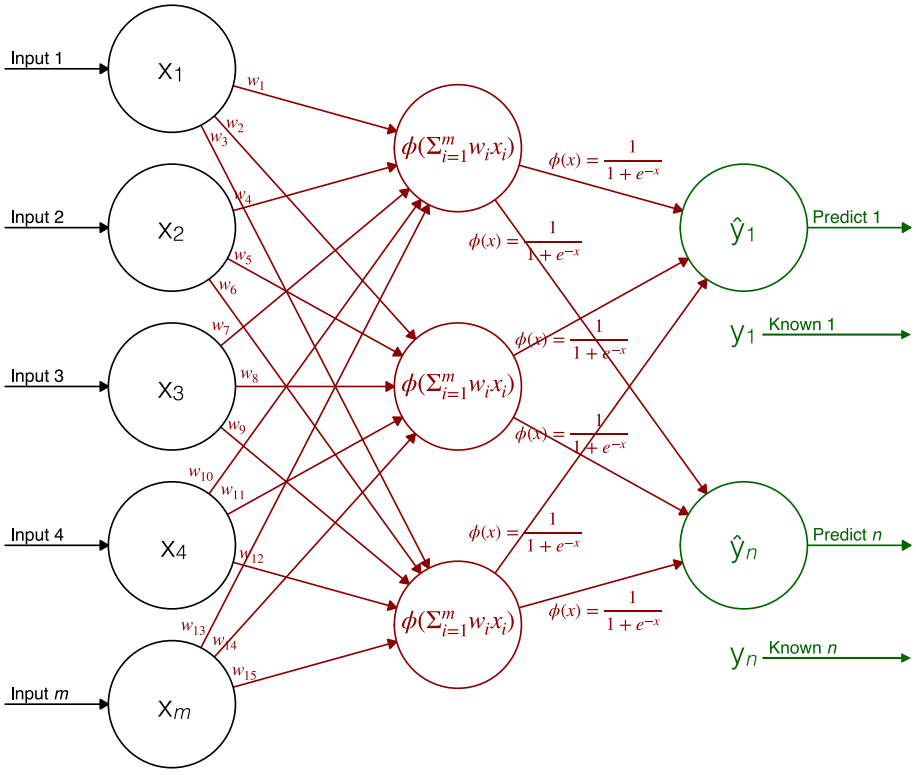

Fig. 1. A generic representation of a multi-label classification artificial neural network. The input layer (black, left) shows five nodes, each representing a unique set of input information; the hidden layer (red, center) is made up of three nodes performing a mathematical transformation; and the output layer (green, right) shows two nodes representing two distinct categories. (For interpretation of the references to colour in this figure legend, the reader is referred to the Web version of this article.)

threshold, the artificial neural network revises the synapse weights by retracing the influence of each input throughout the model using a process called "backpropogation" (Hecht-Nielsen 1992). The weights are revised—informed by the results of the previous training iteration—and the model repeats the training process. The training process is repeated until the sum of squared errors is less than the pre-defined error threshold. This iterative process ultimately "discovers intricate structure in large data sets" (LeCun et al., 2015: 436) that precisely captures the underlying relationships between the input and output information originally provided to the artificial neural network (Braspenning 1995).

2.1. *Artificial neural networks in an archaeological research context*

In an archaeological context, we can employ artificial neural networks to model patterns between the composition of artifact assemblages and known dates of occupation by mimicking the thought processes of archaeologists in the field when "instinctively" recognizing general periods of site occupation based on visible artifacts on the contemporary ground surface. When this identification process is occurring, we are using our own cognitive "neural networks" to determine the time periods a site was likely occupied. This happens by observing the information available to us, performing unobservable calculations within our minds that take into account all prior knowledge of similar observations, and then producing a possible conclusion. If that initial conclusion does not match with all of the information that we have observed, we quickly reassess. This process is completed an unknown number of times until we are satisfied that our conclusions are reasonably supported by the observations we make on-the-ground (Krenker et al., 2011; Wang 2003).

An artificial neural network functions much in the same way by assessing and reassessing input and output information, but can iterate and record the process billions of times over, ultimately producing far greater predictive precision than we could ever expect to produce through our own cognitive neural networks. Employing the computational power of artificial neural networks, therefore, provides an opportunity to use already-established relationships between artifact assemblages and dates of occupation—defined using destructive absolute dating techniques—to predict occupation of archaeological sites using only surface artifact assemblages to a greater precision than we could achieve using only our own cognitive neural networks. The following case study will illustrate the efficacy, accuracy, and predictive power of this deep learning algorithm.

3. An artificial neural network application in the central Mesa Verde region

The central Mesa Verde region in the northern US Southwest (Fig. 2)

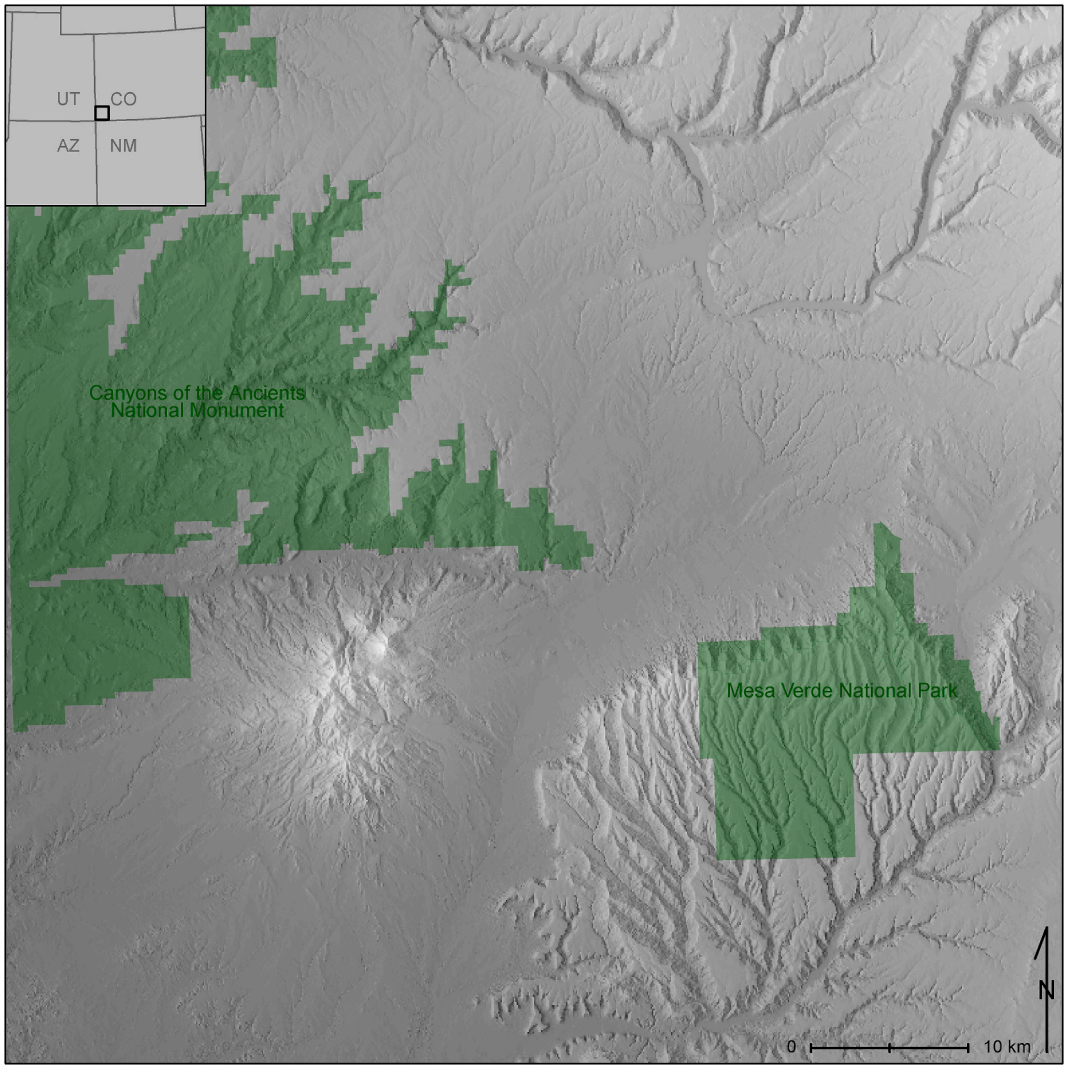

Fig. 2. The central Mesa Verde region. Includes Mesa Verde National Park and Canyons of the Ancients National Monument (shaded in green), located in southwestern Colorado (inset, top left). (For interpretation of the references to colour in this figure legend, the reader is referred to the Web version of this article.)

is an arid, high-desert environment that was continuously occupied by ancestral Pueblo people from 6500 BCE through AD 1300 (Lipe et al., 1999). Little detail is known about population levels prior to AD 575, but population density began to increase around AD 600 and continued (Varien et al., 2007; Wilshusen 1999; Wilshusen et al., 2012)—albeit inconsistently (Ahlstrom et al., 1995; Mahoney et al., 2000; Ortman et al., 2007; Schwindt et al., 2016; Varien et al., 2007)—until the central Mesa Verde region became the most densely populated area in the northern US Southwest during the AD 1100s and 1200s (Glowacki 2015). Despite this established history of occupation, the region was completely depopulated around AD 1300 due to compounding environmental and sociopolitical factors (Benson and Berry 2009; Cameron 2010; Glowacki 2015; Kohler et al, 2010, 2014; Schwindt et al., 2016; Spielmann et al., 2016; Varien 2010).

The central Mesa Verde region is an ideal case study to explore the utility of using artificial neural networks with archaeological datasets because a long history of survey, excavation, and other research efforts in the area (Ortman et al., 2012; Schachner et al., 2012) have already established strong relationships between changes in ceramic construction and decoration with specific temporal ranges (Blinman 2009; Breternitz et al., 1974; Christenson 1994; Crown 2006; Hayes 1964; Hegmon et al., 1997; Kent 1986; Mills 1999; Ortman et al., 2007; Peeples et al., 2016; Rohn 1977; Rohn and Swannack, Jr. 1965; Schwindt et al., 2016; Severance 2015; Sullivan, III et al., 1995; Toll and McKenna 1987; Wilson 1996; Wilson and Blinman 1995). These relationships, initially defined through destructive dating techniques, have already been used in conjunction with changes in architectural construction to predict probabilities of site occupation without the need for collection or excavation (Glowacki and Ortman 2012; Lipe 1989; Lipe et al., 1999; Varien 1999; Wilshusen 2018). Varien et al. (2007), later followed by Schwindt et al. (2016), implemented a Bayesian analysis to utilize the "prior knowledge" of these temporal relationships to calculate the probability of site occupation in each of 14 modeling periods from AD 600–1280 (Ortman et al., 2007). Probabilities of occupation were calculated by employing prior knowledge of ceramic, architectural, and observational information at sites with known occupation spans, and extrapolating the relationships between each of these lines of evidence to estimate occupation at sites with no known dates of use (Ortman et al., 2007). While the model presented here uses the same dataset as these previous analyses by Varien et al. (2007) and Schwindt et al. (2016), the analytical focus is put explicitly on the temporal relationship between ceramic assemblages and dates of occupation. By shifting the focus to creating a model requiring only tallies of surface ceramic assemblages to accurately predict periods of occupation, ideally, future surveys need only record frequencies of visible ceramic types if the goal is strictly to determine likely years of use.

Several projects in the central Mesa Verde region have already implemented the type of data collection necessary to predict site occupation at newly-recorded and revisited sites (for example Glowacki 2012; Glowacki et al., 2017; Reese 2018, 2019, 2021; Varien and Coffey 2017). The typical process involves identifying a concentration of surface artifacts associated with each site, typically within the site midden, and delineating a 3-m diameter circle with pin flags (Glowacki and Ortman 2012). All ceramic types within the circle are identified and frequencies recorded. Once the process is completed, and the pin flags are removed, there is no lasting trace of any data collection activity in the area. This same general process can be implemented elsewhere with data collection tailored to artifacts indicative of occupation within the local study region.

3.1. Preparing the dataset

The archaeological database used in this analysis was assembled by the Village Ecodynamics Project (VEP; Kohler et al., 2010; Kohler 2012)—a multi-year and multi-institutional research collective funded by the National Science Foundation—that aggregated information from all known archaeological sites in the central Mesa Verde region recorded over the past century. The aggregated information includes site locations, artifact assemblages, architectural characteristics, and all available tree-ring dating information (Kohler and Varien 2012; Kohler et al., 2010; Ortman et al., 2007; Schwindt et al., 2016; Varien et al., 2007). This database includes approximately 9000 archaeological sites, most with corresponding ceramic and architectural data, and almost 4000 cutting and near-cutting tree-ring dates. All sites in this database that have both ceramic tallies and cutting or near-cutting tree-ring dates are used to train the artificial neural network, but the trained model is later used to predict only occupation of residential structures with no known dates of occupation to create an annual demographic reconstruction of the central Mesa Verde region from AD 450–1300.

3.1.1. Ceramics

While the VEP database is rich in information, it also builds on more than a century of archaeological inquiry—including legacy data that reflects evolving artifact typologies, classification categories, and estimated date ranges of production (Breternitz et al., 1974; Wilson and Blinman 1995). The evolution of ceramic typologies over the past century means certain classifications were introduced, used, abandoned, or selectively used through time (for example Hayes 1964; Rohn and Swannack, Jr. 1965). Therefore, the ceramic dataset had to be standardized using contemporary categories of ceramic typologies to make the model broadly applicable to all sites within the central Mesa Verde region recorded over the past century. This process generally included renaming some types of ceramics when the category had changed, combining columns of data for those that had been subsumed by others, and removing ceramic types that have been inconsistently recorded through time. Some ceramic types from the central Mesa Verde typology were also removed from this analysis because they are considered "non-diagnostic" categories that do not represent a specific time-period, but rather an era of production. The complete list of ceramic types used in this analysis, along with corresponding maximum estimated date ranges of production, is shown in Table 1 (all ceramic typologies and corresponding resources for dates of production are provided in Supplemental Table 1).

Once the ceramic typologies were standardized across the database, and non-diagnostic ceramic wares were removed, sites with multiple ceramic tallies were collated. This created a large table with each row representing one site, and each column representing the total frequencies of each ceramic type identified at the corresponding site. The collated tallies were then normalized within each site assemblage by re-scaling the raw ceramic counts to values between 0 and 1 (LeCun et al., 1998). Normalized ceramic data are used instead of raw counts because these re-scaled values are directly comparable between sites regardless of the total number of ceramics identified. It is these normalized values of ceramic types that are later considered in conjunction with tree-ring dates to train the artificial neural network; and eventually used to predict periods of site occupation for residential structures using only a tally of ceramic types. Ultimately, this means the trained artificial neural network is broadly applicable to all ceramic assemblages whether one or thousands of ceramics were counted at a given site—because the model need only consider proportions between ceramic types. This step is important as the goal is to apply the model to all previously recorded ceramic assemblages in the database, along with all surface assemblages recorded in the future, regardless of the raw number of ceramics within a given assemblage.

3.1.2. Tree-rings

The extensive collection of cutting and near-cutting tree-ring dates from the central Mesa Verde region, also compiled by the VEP, provides a highly detailed snapshot of construction activity and occupation for specific sites in specific years. Residential structures, however, are typically occupied longer than the year(s) in which they were constructed. The tree-ring dataset was modified to reflect likely extents of

Table 1
Ceramic type names and corresponding maximum date ranges of production used in training and implementing the artificial neural network. All resources considered for each date range are provided in Supplemental Table 1.

Ceramic type name	Maximum production range (AD)	Resources
Chapin/Fugitive/ Lino/Twin Trees Gray	450–980	Breternitz et al. (1974); Ortman et al. (2007); Wilson and Blinman (1995)
Moccasin Gray	775–980	Breternitz et al. (1974); Ortman et al. (2007); Rohn (1977); Wilson and Blinman (1995)
Mancos Gray	850–1060	Breternitz et al. (1974); Mills (1999); Ortman et al. (2007); Wilson and Blinman (1995)
Dolores Corrugated	1025–1300	Mills (1999); Ortman et al. (2007); Severance (2015); Wilson and Blinman (1995)
Mesa Verde Corrugated	1100–1300	Breternitz et al. (1974); Mills (1999); Ortman et al. (2007); Wilson and Blinman (1995)
Abajo Red-on-orange	700–880	Christenson (1994); Hegmon et al. (1997) Ortman et al. (2007); Wilson and Blinman (1995)
Bluff Black-on-red	750–950	Christenson (1994); Hegmon et al. (1997) Ortman et al. (2007); Wilson and Blinman (1995)
Deadman's Black-on-red	780–1100	Christenson (1994); Hegmon et al. (1997) Ortman et al. (2007); Wilson and Blinman (1995)
Chapin Black-on-white	575–900	Breternitz et al. (1974); Ortman et al. (2007); Rohn (1977); Wilson and Blinman (1995)
Piedra Black-on-white	750–920	Breternitz et al. (1974); Ortman et al. (2007); Rohn (1977); Wilson and Blinman (1995)
Cortez Black-on-white	880–1060	Breternitz et al. (1974); Kent (1986); Ortman et al. (2007); Wilson and Blinman (1995)
Mancos/Wetherill Black-on-white	900–1180	Breternitz et al. (1974); Hayes (1964); Ortman et al. (2007); Rohn (1977); Wilson (1996) Wilson and Blinman (1995)
McElmo Black-on-white	1050–1300	Breternitz et al. (1974); Ortman et al. (2007); Rohn (1977); Wilson and Blinman (1995)
Mesa Verde Black-on-white	1150–1300	Breternitz et al. (1974); Ortman et al. (2007); Rohn (1977); Wilson and Blinman (1995)

occupation at each site based on the estimated use-life of residential structures. Varien and colleagues (2007: Table 3) present use-life estimates from AD 600–1280 in the central Mesa Verde region for both small isolated residential structures ("small sites," Varien and Ortman 2005), and those located within large aggregated community centers ("village sites," Kohler 1988; Wilshusen 1986)—identified by their inclusion in the community center database (Adler 1996; Duff and Wilshusen 2000; Glowacki and Ortman 2012; Lipe and Ortman 2000; Lipe et al., 1999; Mahoney et al., 2000; Ortman et al. 2000, 2012; Varien 1999; Varien et al., 1996; Varien and Wilshusen 2002). The use-life estimates compiled by Varien et al. (2007) are used here, although the estimates are extended to the entire AD 450–1300 study period. Use-life estimates for residential structures in AD 600 were extended back to AD 450 for the purposes of this analysis, and years after AD 1280 were assigned an incrementally declining use-life estimate so no occupations were present by the year AD 1300. These residential use-life estimates were incorporated into the tree-ring dataset by adding presence values (1) to the corresponding number of subsequent columns equal to the estimated use-life of a given residential structure. For example (illustrated in Table 2), a tree-ring cutting date of AD 673 at a small residential site would suggest a use-life of 8 years (Varien et al., 2007: Table 3); therefore a tally in each of the "673" through "680" columns would be added. If there was a second tree-ring cutting date of AD 679 at the same site, then another presence value (1) was added to the "679" through "686" columns.

Similar to the ceramic dataset, all tree-ring counts were then collated by site. Returning to the example in Table 2, combining the tree-ring dates with estimated years of residential use-life at example site "A" would suggest a total occupation span from AD 673–686, and provide a signal to the artificial neural network to center a likely occupation around AD 679–680. This process was repeated for all available cutting and near-cutting tree-ring dates, creating two large tables—one to predict small site occupation and the other to predict village site occupation—where each row represented a single site and each column represented the summed tree-ring dates and estimated extents of occupation.

3.1.3. Training and test datasets

The resulting ceramic and tree-ring datasets were then aggregated by site number. The final datasets include a total of 118 sites for which both ceramic tallies and tree-ring dates were available. The aggregated small site and village site datasets with known input (normalized ceramic values) and output (tree-ring frequencies) information were then used to train and test two separate artificial neural networks by splitting each dataset into two subsets: 80% of sites were randomly selected to be in a training dataset, which is "a set of examples used for learning, that is to fit the parameters of the classifier" (Ripley 1996: 354), and; the remaining 20% of sites were assigned to a test dataset, which is "a set of examples used only to assess the performance of a fully-specified classifier" (Ripley 1996: 354).

Each artificial neural network is first trained using the training dataset, and then the trained model is applied to the corresponding test dataset. Predicted results from the test dataset are then used to calculate model accuracy for each year from AD 450–1300, and the average predictive accuracy of the model across the entire study period, by directly comparing the predicted results with corresponding known

Table 3
Refined Pecos Classification ranges and exploration/exploitation transition year for each time period. Dates prior to AD 470 and after AD 1295 are intentionally left blank because they are beyond the scope of data available for this analysis. Bocinsky et al. (2016) report similar date ranges (AD): 500–700 (Basketmaker III), 700–890 (Pueblo I), 890–1145 (Pueblo II), and 1145–1285 (Pueblo III); with transitions from exploration to exploitation in 600, 790, 1035, and 1200, respectively.

Time Period	Begin (AD)	Explore/Exploit (AD)	End (AD)
Basketmaker II			470
Basketmaker III	470	600	710
Pueblo I	710	790	890
Pueblo II	890	1035	1145
Pueblo III	1145	1200	1295
Pueblo IV	1295		

Table 2
Example site "A" with two known tree-ring cutting dates of AD 673 and 679, and the total extent of occupation used for training the artificial neural network.

Site ID	Cutting date (AD)	450–672	673	674	675	676	677	678	679	680	681	682	683	684	685	686	687–1300
A	673	0	1	1	1	1	1	1	1	1	0	0	0	0	0	0	0
A	679	0	0	0	0	0	0	0	1	1	1	1	1	1	1	1	0
Total		0	1	1	1	1	1	1	2	2	1	1	1	1	1	1	0

dates of occupation.

3.2. Training and testing the artificial neural network

While the researcher cannot directly control the production of a deep learning model, the parameters of the model can be manipulated to produce the best possible results. This includes defining the input information, output information, error threshold, model repetitions, and the maximum number of iterations the algorithm should run before declaring a failure to converge (using R package "neuralnet"; Fritsch et al., 2019). The most difficult parameter to define, however, is the number of nodes within the hidden layer. Despite a large number of publications offering guidelines to determine the optimal number of hidden nodes for a given dataset (for example Berry and Linoff 1997; Blum 1992; Boger and Guterman 1997; Huang et al., 2010; Odikwa et al., 2020; Panchal and Panchal 2014; Stathakis 2009; Swingler 1996), there is no consensus on the correct method for this process. While determining the optimal number of hidden nodes is ideal, it is most important to avoid drastically over-training or under-training the model. Over-training an artificial neural network (by allowing too many hidden nodes) will result in a model tailored only to the training dataset, limiting its broad applicability (Astion et al., 1993). Similarly, under-training a model (by employing too few hidden nodes) results in an artificial neural network that is not robust enough to make informed predictions when applied beyond the training dataset (Fletcher et al., 1998). Blum (1992) suggests the number of hidden nodes in an artificial neural network should fall between the input and output layer sizes. This rule-of-thumb was used to create and test a large number of models with the full range of possible hidden nodes to find the most accurate model for the archaeological data from the central Mesa Verde region. The number of nodes in the input layer for these models is 14—each representing a diagnostic ceramic type (Table 1)—and the number of nodes in the output layer is 851—one for each year from AD 450–1300. Therefore to determine the optimal number of nodes for the small site and village site datasets, a brute-force approach of training and testing 837 artificial neural networks for each model with 14–851 nodes in the hidden layer was done to determine the optimal number of hidden nodes for each dataset. The same training and test datasets were used for each model iteration so the accuracy between the trained models would be directly comparable (all R code used in this project is available on Github).

Each iteration of the trained artificial neural network was then applied to the test dataset. After calculating the initial predictions of occupation, two calculations were made to further refine the results:

1. Possible years of occupation were limited by the maximum date range of production for the ceramic types present within each site assemblage (Table 1). For example, if a site only had Mesa Verde Black-on-white in the assemblage, then the distribution of predictions for a site was limited to AD 1150–1300 (Breternitz et al., 1974; Rohn 1977; Wilson and Blinman 1995). Conversely, if both Chapin Gray and Mesa Verde Black-on-white were within a site assemblage, then the distribution of predictions for that site could span the total AD 450–1300 range (Breternitz et al., 1974; Rohn 1977; Wilson and Blinman 1995). This was done to limit the influence of sites in the training dataset that may have had multiple occupation components, possibly creating a relationship within the trained model between later ceramic typologies and earlier years, or vice versa. After limiting the years of possible occupation to the maximum range of ceramic production, the predictions were redistributed over the remaining years by normalizing the initial values—creating a stronger signature of occupation where it likely existed, and removing the possibility of unlikely occupations.
2. The redistributed values were run through a Gaussian smooth with a varying window size. This was done to decrease the number of "orphan years," where several years around a given year are predicted to have an occupation, but one year does not. While moving away from a residence for one year is certainly possible, the orphan year is more likely the byproduct of an unintended relationship created between specific ceramic assemblages with specific years in the training dataset. For example, perhaps there are no recorded dates of occupation for a specific year within the training dataset, and therefore, no corresponding ceramic assemblage would identify an occupation in that specific year. Predicted results from each iteration of the artificial neural network were smoothed with windows of 1 (no smooth) to 50 to determine the optimal smoothing window for each dataset.

The predicted results of the test datasets were then directly compared to the corresponding known dates of occupation for each site. Fig. 3 shows: the predictive accuracy for small sites by year using the optimal number of hidden nodes and optimal smoothing window size for the AD 450–1300 study period (top, red); the predictive accuracy for village sites by year using the optimal number of hidden nodes and optimal smoothing window size for the AD 450–1300 study period (middle, red); the corresponding lower and upper bounds of the 95% confidence interval for each model in each year (gray); and the number of cutting and near-cutting tree-ring dates supporting the model for each year (bottom, purple). A plot showing the Area Under the Curve (AUC) for the optimal models is also provided in Supplemental Figure 1 (small sites, $AUC = 0.947$) and Supplemental Figure 2 (village sites, $AUC = 0.941$).

For the small sites dataset, the optimal number of nodes within the hidden layer is 18, and the optimal smoothing window is 21—meaning the model produced the most accurate results when the smoothing window applied to the predictions was similar to the average use-life of a small site residential structure across the entire study period (average use-life from AD 450–1300 was approximately 19 years). This combination creates an artificial neural network with a minimum 72.4% accuracy, and an average annual predictive accuracy of 93.5% for the AD 450–1300 study period. (K-fold cross-validation with 5-folds and repeated 10 times results in an average accuracy of 90.9% using the optimal number of hidden nodes and optimal smoothing window for small site residential structures.)

For the village sites dataset, the optimal number of nodes within the hidden layer is 16, and the optimal smoothing window is 36—again, the most accurate results were produced when the smoothing window was similar to the average use-life of a village site residential structure (average use-life from AD 450–1300 was approximately 31 years). This combination creates an artificial neural network with a minimum 69% accuracy, and an average annual predictive accuracy of 92.1% for the study period. (K-fold cross-validation with 5-folds and repeated 10 times results in an average accuracy of 89.8% using the optimal number of hidden nodes and optimal smoothing window for village site residential structures.)

3.3. Applying the trained model to the central Mesa Verde database

Once the optimal parameters for each model were identified, the trained artificial neural networks were applied to sites across the central Mesa Verde region with a residential component. Of the 7600 recorded sites with a residential component, approximately 60% have a corresponding ceramic tally reporting frequencies of ceramic types, approximately 20% have a ceramic tally that does not report any diagnostic wares or only reports the presence/absence of various ceramic types, and approximately 20% have no reported ceramic information. This means occupation can be predicted for 60% of sites in the central Mesa Verde region using the trained artificial neural networks, but other steps must to be taken to account for the remaining 40% of sites.

Small sites that had ceramic tally information without diagnostic wares, alongside sites with presence/absence ceramic type information, were assigned the occupation predictions of the closest neighboring small site that best matched the reported ceramic assemblage. This process required using the maximum estimated date ranges of

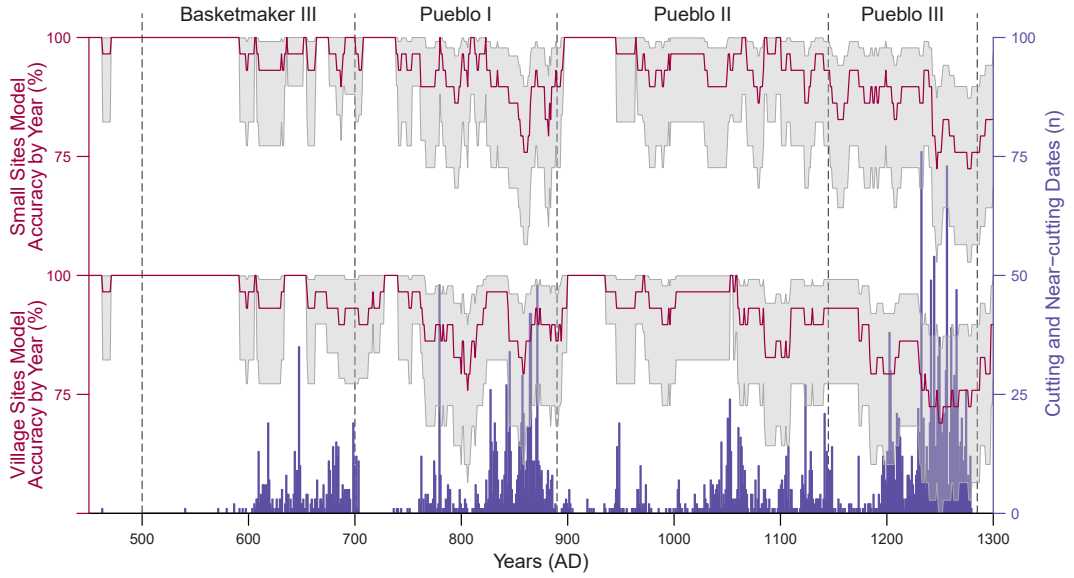

Fig. 3. Model accuracy by year. The accuracy of the optimal small sites artificial neural network by year from AD 450–1300 (top, red), the accuracy of the optimal village sites artificial neural network by year from AD 450–1300 (middle, red), and the corresponding 95% confidence intervals (gray). The figure also shows the number of cutting and near-cutting tree-ring dates, by year, used to support the model (bottom, purple). The vertical dashed lines are recently refined Pecos Classification periods for the central Mesa Verde region (Bocinsky et al., 2016). (For interpretation of the references to colour in this figure legend, the reader is referred to the Web version of this article.)

production for all ceramic wares (diagnostic and non-diagnostic, provided in Supplemental Table 1) and applying a tally to each year from AD 450–1300 corresponding to the possible ranges of production for each ceramic type reported at each site. Once all ceramic wares at each site were tallied across the study period, the years with the maximum values were identified—representing the years with the most overlap in estimated date ranges of production for the reported ceramic assemblage. These small sites were then assigned the predicted occupation of the closest neighboring small site—based on Euclidean distance—with which the occupation prediction fell within the range of years identified as having the most ceramic production overlap. Therefore, the occupation predictions assigned to small sites with limited ceramic information are strictly bound by the most likely periods of site occupation based on each reported ceramic assemblage. Small sites without any ceramic information were distributed across the study period based on annual predicted residential occupation density through time. Therefore more households with unknown ceramic information were added to years with greater predicted residential site occupation, while proportionally less were added to years with smaller predicted residential site occupation.

Village sites that do not contain diagnostic wares within the ceramic tally, or those without ceramic tally information altogether, were assigned the occupation predictions of the closest neighboring village site—based on Euclidean distance—with ceramic or tree-ring dating information. While this solution may not perfectly reflect the reality on the ground, assuming spatially clustered residences within a community center are occupied contemporaneously is consistent with the assumption that households choose to live near one another to maintain regular interaction within a community (Peterson and Drennan 2005, 2011; Reese et al., 2019; Varien 1999), and is further consistent with previous demographic reconstructions in the central Mesa Verde region (Ortman et al., 2007; Varien et al., 2007). The resulting predictions provide annual snapshots of household density and movement (Fig. 4).

Fig. 4 shows the annual density distribution of occupied residences in the central Mesa Verde region from AD 1055–1060 as predicted by the trained artificial neural networks. The power in this analysis is the degree of predictive accuracy, coupled with the spatial precision of the dataset, to estimate periods of site occupation. Fig. 4 illustrates incremental changes in the density of residential occupation at a regional scale, slowly dispersing in some areas while simultaneously aggregating in others, revealing a resolution of population movement that would otherwise be impossible without collecting and analyzing dendrochronological samples at every recorded residential site across the central Mesa Verde region. Future applications of this model can employ the available spatial and temporal precision to observe intra-community population changes, and intra-regional migration events through time.

3.4. Reconstructing demography

Annual predictions of residential site occupation were then used to calculate numbers of households and total population estimates for the central Mesa Verde region from AD 450–1300. While “residences” are the physical architecture representing domestic activity, “households” in the central Mesa Verde region are considered “minimal social units” (Lightfoot 1994: 12) that represent approximately 3.3–7 people (Kohler 2012; Lightfoot 1994; Ortman et al., 2007; Schwindt et al., 2016). The number of households at a residential site are typically counted by the corresponding number of recorded pitstructures (Lekson 1988; Lightfoot 1994; Lipe 1989; Ortman et al., 2007; Varien 1999), but all pitstructures at a site are not necessarily occupied contemporaneously. Ortman and colleagues (2007: Figure 8) examined the variable length of occupation at several excavated sites in the central Mesa Verde region and determined “the longer the occupation span, the lower the ratio between the peak population and total pit structures for these sites” (Ortman et al., 2007: 262). To incorporate this general pattern of behavior in the demographic reconstruction presented here, a rate of peak population decay was calculated to determine the maximum number of contemporaneously occupied residences at sites with more than one recorded pitstructure.

3.4.1. Calculating peak residential occupation

Peak population decay was calculated from three excavated sites (Grass Mesa Village, Yellow Jacket Pueblo, and Castle Rock Pueblo) in the central Mesa Verde region with known lengths of occupation, total numbers of pitstructures, and the known maximum number of

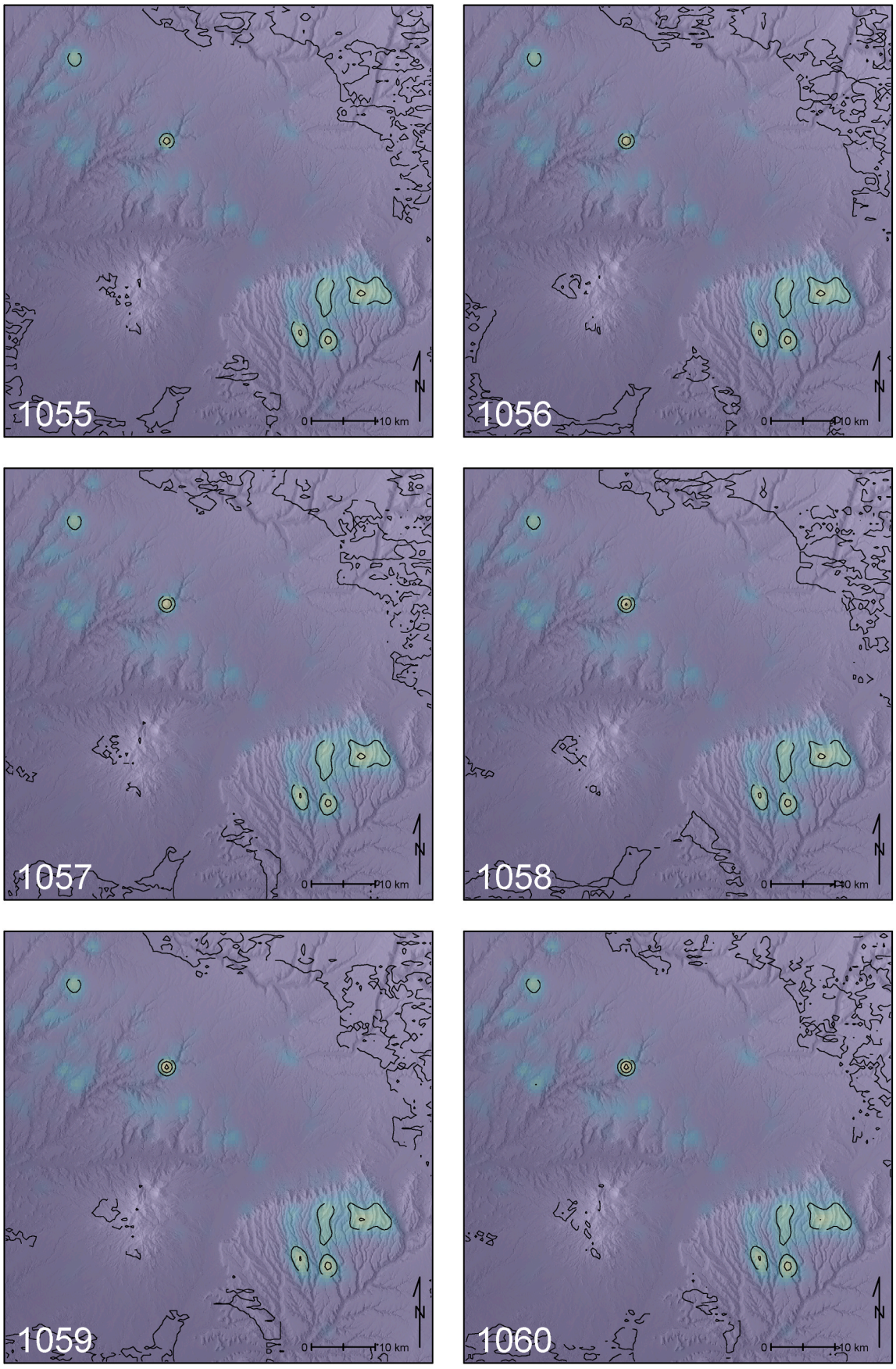

Fig. 4. Residential density distribution. Annual density distribution of occupied residences in the central Mesa Verde region for six years: AD 1055, 1056, 1057, 1058, 1059, and 1060.

contemporaneously occupied pitstructures (Ortman et al., 2007: Figure 8). The proportion between maximum number of contemporaneously occupied pitstructures and total numbers of pitstructures was divided by the total length of occupation at each of these three sites. The result is the decreasing rate of contemporaneously occupied pitstructures per year of total site occupation—or, the rate of peak population decay (calculated decay rates by excavated example site are available in Supplemental Table 2). The rate of peak population decay is multiplied by the total number of years a residential occupation is predicted by the artificial neural network. The total rate of peak population decay is then multiplied by the total pitstructures recorded at each site, and that value is subtracted from the total number of recorded pitstructures to determine the maximum number of contemporaneously occupied pitstructures—the peak population. Numbers of households are then apportioned across the occupation range of each site by multiplying peak population by the probability of occupation determined by the artificial neural network. This creates a distribution of the number of households occupying each residential structure in any given year throughout the total occupation span of that site; and apportions the peak population to the years in which the probability of occupation at each structure is greatest.

3.4.2. *Extrapolating recorded residential structures to unsurveyed areas*

Despite the long history of archaeological inquiry, the majority of the central Mesa Verde region remains unsurveyed (approximately 80%, surveyed areas shaded in Fig. 5a). Therefore the extent of occupation identified by the artificial neural network is limited to previously-recorded residential structures, and does not represent the full extent of population across the central Mesa Verde region from AD 450–1300. To account for residences that likely exist beyond current survey boundaries, a predictive model (using R package "randomForest"; Liaw and Wiener 2002) was created to identify areas across the central Mesa Verde region that would most likely be occupied by similar residential sites through time. This model assumes (following Schwindt et al.,

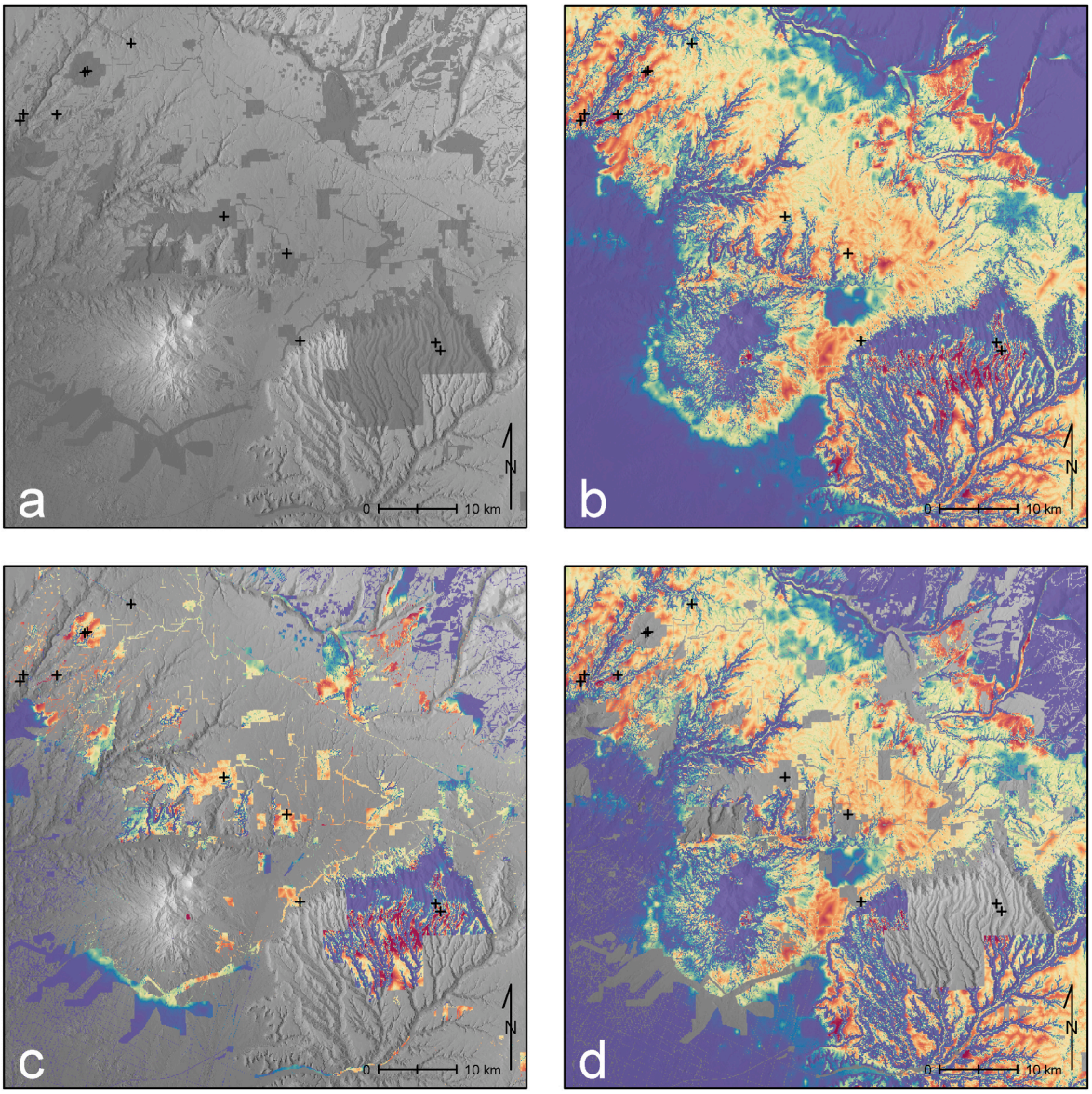

Fig. 5. Extrapolating unrecorded residential structures. A) the central Mesa Verde region with surveyed areas (shaded in gray) and known residential structures with four pitstructures predicted to be occupied to some degree in AD 1060 (black); b) a trained predictive raster for the entire central Mesa Verde region based on known residential site locations showing cells most- (red) to least-likely (purple) to contain a residential structure with four pitstructures occupied to some degree in AD 1060; c) the predictive raster shown within previously-surveyed areas; and d) the predictive raster shown in unsurveyed areas of the central Mesa Verde region. (For interpretation of the references to colour in this figure legend, the reader is referred to the Web version of this article.)

2016): 1) all residential structures within recorded community centers are already documented and accounted for within the village sites dataset; 2) all structures with ≥ 9 pitstructures are already recorded and accounted for within the dataset; 3) all residential structures within surveyed boundaries have been recorded, and; 4) site density, by structure size, is constant across all cells with the same topographic and environmental characteristics for any given year.

The predictive model is run iteratively for each size of small site residential structure ranging from 1 to 8 pitstructures within each year from AD 450–1300. In years with no predicted occupation, based on the results from the small sites artificial neural network, zero (0) occupied residences are predicted to exist in unsurveyed areas. In years with no predicted occupation within a residential structure with a certain number of pitstructures, zero (0) residences of that size are predicted to exist in unsurveyed areas. For years with a predicted occupation within surveyed boundaries, a predictive model is used to determine the likely number of same-sized residential structures in unsurveyed areas. This process is illustrated in Fig. 5 using the example year AD 1060 and residential sites with four pitstructures, and is summarized:

- All recorded sites with four pitstructures that are assigned at least one household occupying the residential structure during AD 1060 are subset from all other sites (Fig. 5a);
- A predictive model is constructed using nine layers at a 10 m resolution, and include:
  1. A digital elevation model (U.S. Geological Survey and EROS Data Center, 1999);
  2. The slope of the terrain (using R package “raster”; Hijmans 2020);
  3. The aspect of the terrain (using R package “raster”; Hijmans 2020);
  4. The direction of water flow (using R package “raster”; Hijmans 2020);
  5. The accumulated cost-distance to ephemeral drainages (using R package “gdistance”; van Etten 2017);
  6. The accumulated cost-distance to permanent water sources (using R package “gdistance”; van Etten 2017);
  7. The mean of annual temperature for the previous 20 years to reflect perceived environmental conditions through time (in the example case, from AD 1040–1060; using R package “paleocar”; Bocinsky 2019; Bocinsky and Kohler 2014; Jha et al., 2018; Marin 2010; West et al., 2008);
  8. The mean of annual precipitation for the previous 20 years to reflect perceived environmental conditions through time (using R package “paleocar”; Bocinsky 2019; Bocinsky and Kohler 2014; Jha et al., 2018; Marin 2010; West et al., 2008); and
  9. The mean of annual maize growing niche for the previous 20 years to reflect perceived availability of food resources through time (using R package “paleocar”; Bocinsky 2019; Bocinsky and Kohler 2014; Jha et al., 2018; Marin 2010; West et al., 2008);
- The recorded locations of each residential site with four pitstructures are used to train the predictive model (Fig. 5b);
- All cells of the trained predictive model within previously-surveyed areas are isolated from the unsurveyed areas (Fig. 5c);
- The value of each cell in the trained predictive model with an occupied residential site is extracted, and the mean value of those cells is calculated;
- The number of cells containing an occupied residential site is divided by the total number of surveyed cells with a predictive value greater than or equal to the mean value of cells with an occupied residential site—creating a proportion of knowingly occupied cells to all surveyed cells with similar topographic and environmental characteristics;
- All unsurveyed cells of the trained predictive model are isolated from previously-surveyed areas (Fig. 5d);
- The number of unsurveyed cells with a predictive value greater than or equal to the mean value of cells with an occupied residential site within surveyed areas is calculated, and multiplied by the proportion of knowingly occupied cells to all cells within surveyed areas with similar topographic and environmental characteristics—resulting in the likely number of residential structures with four pitstructures that exist beyond current survey boundaries that were occupied to some degree in AD 1060;
- The number of predicted residential structures is multiplied by the mean number of households occupying recorded residential structures with four pitstructures during the year AD 1060 as predicted by the trained artificial neural network;
- The result is the number of households that likely occupied a residential structure with a total of four pitstructures beyond survey boundaries during AD 1060—in this example case, there are likely 25 sites with four pitstructures in unsurveyed areas within the central Mesa Verde region, which housed 70 households in AD 1060.

This process is repeated for all small sites with 1–8 pitstructures, and for each year from AD 450–1300. The resulting estimated numbers of households that exist beyond current survey boundaries are then added to the household population estimates previously calculated within surveyed boundaries.

3.4.3. *From numbers of households to demographic reconstruction*

To transform numbers of predicted households within residential structures to reflect population through time, the total number of households predicted to exist across the entire central Mesa Verde region were smoothed with a changing window size equivalent to average life-expectancy of the corresponding year (Kohler and Reese 2014). Smoothing the numbers of households by life-expectancy introduces a third variable to inform the total population estimate of the region, arguably creating a more realistic continuity in population size through time that is not strictly reliant on raw counts of residences as a direct proxy for total numbers of people.

4. Results

Results from the artificial neural network analysis, extrapolated to unsurveyed areas and smoothed by life-expectancy, are used to estimate annual population of the central Mesa Verde region from AD 450–1300 (see Supplementary Movie 1 for mapped population density within surveyed areas from AD 450–1300). Fig. 6 shows the raw number of recorded occupied residences as predicted by the artificial neural network (red), and the total numbers of households predicted to exist in the region multiplied by the potential range of people within each household (gray, 3.3–7, from Kohler 2012; Lightfoot 1994, respectively). The total population estimates for the central Mesa Verde region are calculated by multiplying the total predicted households by 6 people per household (black), consistent with previous reconstructions and ethnographic research (Lightfoot 1994; Schwindt et al., 2016; Varien et al., 2007). The results from Schwindt et al. (2016) are also shown for comparison (purple, 3.3–7, from Kohler 2012; Lightfoot 1994, respectively, with a solid line showing 6 people per household), however, the extrapolation method to predict numbers of residential structures in unsurveyed areas used in the analysis presented here is applied to the Schwindt et al. (2016) predictions.

Residential occupation cannot be identified by the artificial neural networks in years prior to AD 571, highlighting the need for more information to predict occupation for those particular years. Years prior to AD 571 and other years with low predicted population, however, align with previously identified years of decreased population in the central Mesa Verde region (Duff and Wilshusen 2000; Schlanger and Wilshusen 1993; Wilshusen and Perry 2008; Wilshusen et al., 2012), suggesting the model is correctly characterizing overall trends in household occupation through time.

Observing changes in population density at an annual timescale can illuminate household-level responses during periods of conflict,

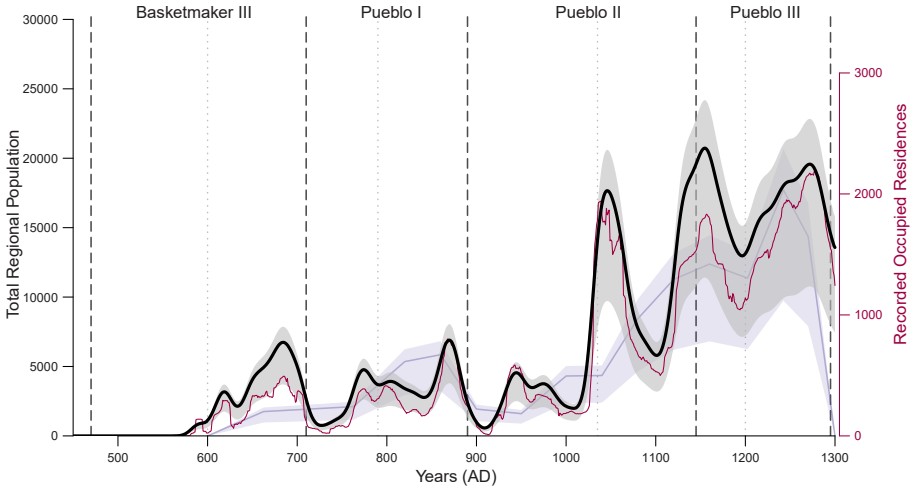

Fig. 6. Demographic reconstruction of the central Mesa Verde region. The predicted annual number of recorded occupied residences in the central Mesa Verde region from AD 450–1300 (red), total numbers of people shown as a range (gray) based on the lowest extent of people per household (3.3, Kohler 2012) and the greatest extent of people per household (7, Schwindt et al., 2016). An estimate with 6 people per household is also presented (black, Lightfoot 1994; Schwindt et al., 2016; Varien et al., 2007). The vertical dashed lines are further refined Pecos Classification periods for the central Mesa Verde region informed by the results of this analysis. Transition years from exploration to exploitation (Bocinsky et al., 2016) for each period are also shown (dotted lines). The purple line (6) and shading (3.3–7) in the background shows population estimates for the central Mesa Verde region calculated by Schwindt et al. (2016)—but using the extrapolation method used in this analysis—and is plotted at the midpoint within each respective modeling period. (For interpretation of the references to colour in this figure legend, the reader is referred to the Web version of this article.)

drought, and sociopolitical changes through time. Fig. 6 shows population estimates that generally align with previously calculated trends, but provide a more precise timescale that reveals intra-period complexities of population growth and decline. Overarching cycles of population growth also align remarkably well with periods of "exploration" and "exploitation" in the central Mesa Verde region (Table 3; Bocinsky et al., 2016). Periods of exploration are years "in which dispersing populations experimented with new settlement locations and new organizational forms [and periods of exploitation are] marked by intensive development of a niche that was simultaneously ecological, cultural, and organizational" (Bocinsky et al., 2016: 1). The alignment between trends in population with periods of exploration and exploitation suggests household investment in building residential structures, and subsequently continuing to occupy them, was strongly tied to successful agricultural productivity. Volatility in agricultural productivity (Bocinsky and Kohler 2014), especially in the earlier Pueblo periods, often led to households shifting locations to increase access to potential resources, and causing periodic fluctuations in population (Schlanger and Wilshusen 1993). Fluctuations in population during the Basketmaker III and Pueblo I periods can be seen in Fig. 6, beginning in earnest around AD 570 and continuing until about AD 915. Cyclical patterns of occupation and abandonment in response to shifts in climatic regimes become less visible in the archaeological record by AD 1000, consistent with correspondingly longer use-lives of residential structures through time (Varien et al., 2007), and suggesting households were generally more sedentary as total population increased in the region. Increased population density meant moving to a productive area as climatic patterns shifted across the region was no longer a viable option for many households to combat periods of poor agricultural productivity (Borck et al., 2015; Cordell et al., 2007; Kohler and Reese 2014; Nelson and Schachner 2002). Potential periods of resource stress were likely offset during this time by intensifying communication and trade networks (Braun and Plog 1982), increasing the use of storage (Burns 1983; Kintigh and Ingram 2018; Spielmann and Aggarwal 2017), and adopting new agricultural technologies (Reese 2020).

A notable population increase centered around AD 1045, decline prior to AD 1100, and subsequent increase in the early AD 1100s departs from recent demographic reconstructions in the central Mesa Verde region (Schwindt et al., 2016; Varien et al., 2007). Part of this discrepancy may be due to the difference in modeling periods, as these studies captured population changes at 40-year intervals from AD 980–1180 (Schwindt et al., 2016: Table 2; Varien et al., 2007: Table 4), presenting results that reflect maximum occupation within each modeling period. However, previous research exploring sedentism and mobility of large, aggregated community centers in the central Mesa Verde region from AD 950–1290 does note a period of demographic downturn and abandonment from AD 1070–1100 (Varien 1999; see also Schlanger and Wilshusen 1993; Varien et al., 1996; Wilshusen and Ortman 1999).

Periods of violence unrelated to corresponding periods of resource stress may provide an explanation for the oscillating population estimates in the late AD 1000s, along with noted periods of population movement and decreased life-exectancy within the northern San Juan region. Kohler et al. (2014) review evidence of bone trauma in the central Mesa Verde region and identify four periods where violence is more prevalent than predicted by contemporaneous resource availability (AD): 1020–1060, 1060–1100, 1140–1180, and 1260–1280 (2014: 453). The authors (Kohler et al., 2014) suggest the initial period of increased violence from AD 1020–1100 reflects local opposition to the growing influence of the Chaco regional system (AD 1040–1135, via Lipe 2006). The demographic reconstruction presented in Fig. 6 suggests violent acts from AD 1020–1100 could have been further exacerbated by a period of increased population density, and abated with a significant decrease in population by AD 1100—a trend reflected in a decreasing juvenility index and decreased life-expectancy in the late AD 1000s (Kohler and Reese 2014). Reese et al. (2019: Fig. 5) also identify a shift in the sociopolitical environment during the AD 1060–1100 period that signals the establishment of new social and economic relationships within communities in the central Mesa Verde region; while Glowacki (2015) notes a period of dramatic population growth within the Totah subregion of the northern San Juan during the AD 1060–1100 period—just south of the central Mesa Verde region presented here—coinciding with the construction of Salmon, Aztec North, and Aztec West greathouses. Therefore the decrease in regional population during the late-AD 1000s was potentially a simultaneous response to the increased period of violence, alongside the re-imagining of socioeconomic relationships as people within the northern San Juan were broadly participating in "reinventing the ceremonial political power of Chaco ideology in the north" (Glowacki 2015: 146). Violence again increased to a level disproportionate to the amount of contemporaneously available resources during the AD 1140–1180 period (Kohler et al., 2014), just as the regional population returned to the same increased levels seen in the AD 1000s. The relationship between population density and periods of violence disproportionate to available resources suggests an upper threshold of social organization in the central Mesa Verde region under Chaco influence that is breached when the population surpasses approximately 15,000 people. Social and cultural

reorganization (Wilshusen and Glowacki 2017), driven by the collapse of the Chaco regional system in the mid-AD 1100s (Lipe 2006), provided an opportunity to "reconceptualize the fundamental aspects of Pueblo culture" (Glowacki 2015: 165) that could better cope with greater population densities. This reorganization resulted in increasingly aggregated communities of people as regional population grew throughout the late AD 1100s and 1200s until reaching an apex of approximately 20,000 people in AD 1272 (Fig. 6, following maximum number of recorded residences). This final increase in regional population corresponds with a final period of increased violence (Kohler et al., 2014) and sociopolitical upheaval (Glowacki 2015) from AD 1260–1280, and this period of violence may have heavily influenced the rate of depopulation from the central Mesa Verde region—as the rate of depopulation from AD 1272–1300 mirrors that of the late AD 1000s. If the rate of population decline was constant from AD 1272, the central Mesa Verde region would have been completely depopulated by AD 1318.

5. Conclusions

By utilizing the known relational information between artifact assemblages and dates of occupation, determined through excavation and absolute dating techniques in the past, a trained artificial neural network becomes a non-destructive and highly accurate tool for dating archaeological sites by predicting site occupation using only tallies of surface artifact assemblages. Artificial neural networks can be broadly applied in other geographic regions as a non-destructive means of archaeological site dating as long as there is a visible component on the contemporary ground surface that is somehow related to a corresponding temporal period. The timescale (or, binning) of models trained in other geographic areas would be equivalent to the accuracy of absolute dates available for the corresponding region of study. For example, a region typically relying on archaeomagnetic dating with confidence intervals spanning 50 years (McIntosh and Catanzariti 2006) can define output nodes in an artificial neural network with 50 year time spans. The resulting trained artificial neural network would then assign occupation to archaeological sites in 50 year increments. The corresponding surface assemblages should, likewise, be chosen to fit the specific study region, but can be any archaeological feature or assemblage that is known to reflect differing temporal periods of site use.

The results produced through the analysis presented here not only offer insight to annual patterns of population growth and decline at a regional scale, but each residence is assigned an independent prediction of occupation. Therefore household movement across the landscape can be observed within specific topographic spaces, ecological zones, aggregated communities, and even between individual residences within a single community. The annual temporal scale, coupled with a precise spatial scale, opens countless opportunities for anthropological research that explores population movement, community aggregation and dispersal, and responses to climatic instability at an annual timescale—or aggregated into larger temporal periods to observe changes in populations on a longitudinal scale.

The method presented here offers an introduction to the application of deep learning artificial neural networks to archaeological site assemblages. Machine learning algorithms can employ vast amounts of legacy archaeological data to predict periods of likely occupation for residential sites recorded in the past, and those yet to be recorded in the future—through non-collection, non-invasive, and non-destructive data collection methods.

Declaration of competing interest

None.

Acknowledgments

This research was made possible with general funding and institutional support provided by the University of Notre Dame and the Santa Fe Institute. The dataset used in this analysis was provided by the Village Ecodynamics Project (supported by the National Science Foundation DEB-0816400 and SMA-1637171). Thank you to the reviewers for their thoughtful feedback and substantive comments that made this paper a more robust and improved version of its original self. The author would also like to thank Mark Golitko, Timothy A. Kohler, Stefani A. Crabtree, and Sean Field for productive discussion and comments.

Appendix A. Supplementary data

Supplementary data to this article can be found online at https://doi.org/10.1016/j.jas.2021.105413.

Funding

This research did not receive any specific grant from funding agencies in the public, commercial, or not-for-profit sectors.

References

Adler, M.A., 1996. Land tenure, archaeology, and the ancestral Pueblo social landscape. J. Anthropol. Archaeol. 15, 337–371.
Ahlstrom, R.V.N., Van West, C.R., Dean, J.S., 1995. Environmental and chronological factors in the Mesa verde-northern rio grande migration. J. Anthropol. Archaeol. 14, 125–142.
Astion, M.L., Wener, M.H., Thomas, R.G., Hunder, G.G., Bloch, B.A., 1993. Overtraining in neural networks that interpret clinical data. Clin. Chem. 39, 1998–2004.
Basu, J.K., Bhattacharyya, D., Kim, T.-h., 2010. Use of artificial neural network in pattern recognition. International Journal of Software Engineering and Its Applications 4, 23–34.
Benson, L.V., Berry, M.S., 2009. Climate change and cultural response in the prehistoric American southwest. KIVA 75, 87–117.
Berry, M.J.A., Linoff, G.S., 1997. Data Mining Techniques. John Wiley & Sons, Inc., New York.
Blinman, E., 2009. Appendix 1: ceramic analysis. In: Cameron, C.M. (Ed.), Chaco and after in the Northern San Juan: Excavations at the Bluff Great House. University of Arizona Press, Tucson.
Blum, A., 1992. Neural Networks in C++: an Object-Oriented Framework for Building Connectionist Systems. John Wiley & Sons, Inc., New York.
Bocinsky, R.K., 2019. *Paleocar: Paleoclimate Reconstruction From Tree Rings Using Correlation Adjusted CorRelation,* R Package, version 4.0.1.
Bocinsky, R.K., Kohler, T.A., 2014. A 2,000-year reconstruction of the rain-fed maize agricultural niche in the US Southwest. Nat. Commun. 5, 1–12.
Bocinsky, R.K., Rush, J., Kintigh, K.W., Kohler, T.A., 2016. Exploration and exploitation in the macrohistory of the pre-Hispanic Pueblo Southwest. Science Advances 2, 1–11.
Boger, Z., Guterman, H., 1997. Knowledge extraction from artificial neural network models. Ieee International Conference on Systems, Man, and Cybernetics. Computational Cybernetics; Simulation, Orlando, 1997.
Borck, L., Mills, B.J., Peeples, M.A., Clark, J.J., 2015. Are social networks survival networks? An example from the late pre-hispanic US southwest. J. Archaeol. Method Theor 22, 33–57.
Braspenning, P.J., 1995. Introduction: neural networks as associative devices. In: Braspenning, P.J., Thuijsman, F., Weijters, A.J.M.M. (Eds.), Artificial Neural Networks: an Introduction to ANN Theory and Practice. Springer Science & Business Media, pp. 1–10.
Braun, D.P., Plog, S., 1982. Evolution of "tribal" social networks: theory and prehistoric north American evidence. Am. Antiq. 47, 504–525.
Breternitz, D.A., Rohn, A.H., Morris, E.A., 1974. Prehistoric Ceramics of the Mesa Verde Region. Museum of Northern Arizona, Flagstaff.
Burns, B.T., 1983. Simulated Anasazi Storage Behavior Using Crop Yields Reconstructed from Tree Rings: A.D. 652–1968, PhD Thesis. University of Arizona, Tucson.
Cameron, C.M., 2010. Advances in understanding the thirteenth-century depopulation of the northern southwest. In: Kohler, T.A., Varien, M.D., Wright, A.M. (Eds.), Leaving Mesa Verde: Peril and Change in the Thirteenth-Century Southwest. University of Arizona Press, Tucson, pp. 346–363.
Casanova, E., Knowles, T.D.J., Bayliss, A., Dunne, J., Barański, M.Z., Denaire, A., Lefranc, P., Lernia, S. di, Roffet-Salque, M., Smyth, J., Barclay, A., Gillard, T., Claßen, E., Coles, B., Ilett, M., Jeunesse, C., Krueger, M., Marciniak, A., Minnitt, S., Rotunno, R., Velde, P., van de, Wijk, I. van, Cotton, J., Daykin, A., Evershed, R.P., 2020. Accurate compound-specific 14C dating of archaeological pottery vessels. Nature 506–510.
Caspari, G., Crespo, P., 2019. Convolutional neural networks for archaeological site detection – finding T "princely" tombs. J. Archaeol. Sci. 110, 104998.

Chase, A.F., Chase, D.Z., Fisher, C.T., Leisz, S.J., Weishampel, J.F., 2012. Geospatial revolution and remote sensing LiDAR in Mesoamerican archaeology. Proc. Natl. Acad. Sci. Unit. States Am. 109, 12916–12921.
Christenson, A.L., 1994. A test of mean ceramic dating using well-dated kayenta anasazi sites. KIVA 59, 297–317.
Colwell-Chanthaphonh, C., 2009. Reconciling American archaeology & native America. Daedalus 138, 94–104.
Conyers, L.B., 2018. Ground-penetrating Radar and Magnetometry for Buried Landscape Analysis. Springer Nature, Switzerland.
Cordell, L.S., Van West, C.R., Dean, J.S., Muenchrath, D.A., 2007. Mesa Verde settlement history and relocation: climate change, social networks, and ancestral Pueblo migration. KIVA 72, 379–405.
Crown, P.L., 2006. Acquisition, use, and discard of red and Brown wares at Pueblo bonito, Chaco canyon. In: Crown, P.L. (Ed.), The Pueblo Bonito Mounds of Chaco Canyon: Material Culture and Fauna. University of New Mexico Press, Albuquerque, pp. 93–122.
Douglas, A.E., 1929. The secret of the southwest solved by talkative tree rings. Natl. Geogr. Mag. 54, 737–770.
Duff, A.I., Wilshusen, R.H., 2000. Prehistoric population dynamics in the northern san juan region, A.D. 950–1300. KIVA 66, 167–190.
Fletcher, L., Katkovnik, V., Steffens, F.E., Engelbrecht, A.P., 1998. Optimizing the number of hidden nodes of a feedforward artificial neural network. In: 1998 Ieee International Joint Conference on Neural Networks Proceedings. IEEE World Congress on Computational Intelligence (Cat. No.98CH36227).
Fritsch, S., Guenther, F., Wright, M.N., 2019. Neuralnet: Training of Neural Networks. R package version 1.44.2.
Glowacki, D.M., 2012. The Mesa Verde Community Center Survey: Final Report. National Science Foundation, Mesa Verde National Park.
Glowacki, D.M., 2015. Living and Leaving: A Social History of Regional Depopulation in Thirteenth-Century Mesa Verde. University of Arizona Press, Tucson.
Glowacki, D.M., Bocinsky, R.K., Reese, K.M., Portman, K.A., 2017. The Mesa Verde Community Center Survey: Summer 2017. Mesa Verde National Park, Cortez.
Glowacki, D.M., Ortman, S.G., 2012. Characterizing community-center (village) formation in the VEP study area, A.D. 600–1280. In: Kohler, T.A., Varien, M.D. (Eds.), Emergence and Collapse of Early Villages: Models of Central Mesa Verde Archaeology. University of California Press, Los Angeles, pp. 219–246.
Hayes, A.C., 1964. The Archaeological Survey of Wetherill Mesa. Mesa Verde National Park, Cortez.
Hecht-Nielsen, R., 1992. Theory of backpropogation neural network. In: Wechsler, H. (Ed.), Neural Networks for Perception, ume 2. Academic Press, San Diego, pp. 65–93. : Computation, Learning, and Architectures.
Hegmon, M., Allison, J.R., Neff, H., Glascock, M.D., 1997. Production of san juan red ware in the northern southwest: insights into regional interaction in early puebloan prehistory. Am. Antiq. 62, 449–463.
Hijmans, R.J., 2020. Raster: Geographic Data Analysis and Modeling.
Huang, G.-B., Ding, X., Zhou, H., 2010. Optimization method based extreme learning machine for classification. Neurocomputing 74, 155–163.
Inomata, T., Triadan, D., López, V.A.V., Fernandez-Diaz, J.C., Omori, T., Bauer, M.B.M., Hernández, M.G., Beach, T., Cagnato, C., Aoyama, K., Nasu, H., 2020. Monumental architecture at Aguada Fénix and the rise of Maya civilization. Nature 1–4.
Jha, C.K., Gupta, V., Chattopadhyay, U., Sreeraman, B.A., 2018. Migration as adaptation strategy to cope with climate change: a study of farmers' migration in rural India. International Journal of Climate Change Strategies and Management 10, 121–141.
Kent, S., 1986. New dates for old pots: a comment on cortez black-on-white. KIVA 51, 255–262.
King, T.F., Lyneis, M.M., 1978. Preservation: a developing focus of American archaeology. Am. Anthropol. 80, 873–893.
Kintigh, K.W., Ingram, S.E., 2018. Was the drought really responsible? Assessing statistical relationships between climate extremes and cultural transitions. J. Archaeol. Sci. 89, 25–31.
Kohler, T.A., 1988. The probability sample at grass Mesa village. In: Lipe, W.D., Morris, J.N., Kohler, T.A. (Eds.), Dolores Archaeological Program: Anasazi Communities at Dolores: Grass Mesa Village. Bureau of Reclamation; Engineering and Research Center, Denver, pp. 51–74.
Kohler, T.A., 2012. Simulation model overview. In: Kohler, T.A., Varien, M.D. (Eds.), Emergence and Collapse of Early Villages: Models of Central Mesa Verde Archaeology. University of California Press, Berkeley, pp. 59–72.
Kohler, T.A., Ortman, S.G., Grundtisch, K.E., Fitzpatrick, C.M., Cole, S.M., 2014. The better angels of their nature: declining violence through time among prehispanic farmers of the Pueblo southwest. Am. Antiq. 79, 444–464.
Kohler, T.A., Reese, K.M., 2014. Long and spatially variable neolithic demographic transition in the north American southwest. Proc. Natl. Acad. Sci. Unit. States Am. 111, 10101–10106.
Kohler, T.A., Varien, M.D. (Eds.), 2012. Emergence and Collapse of Early Villages: Models of Central Mesa Verde Archaeology. University of California Press, Berkeley.
Kohler, T.A., Varien, M.D., Wright, A.M. (Eds.), 2010. Leaving Mesa Verde: Peril and Change in the Thirteenth-Century Southwest. University of Arizona Press, Tucson.
Krenker, A., Bešter, J., Kos, A., 2011. Introduction to the artificial neural networks. In: Suzuki, K. (Ed.), *Artificial Neural Networks - Methodological Advances And Biomedical Applications*, intechweb.Org, pp. 3–18. Rijeka, Croatia.
LeCun, Y., Bengio, Y., Hinton, G., 2015. Deep learning. Nature 521, 436–444.
LeCun, Y., Bottou, L., Orr, G.B., Müller, K.-R., 1998. Efficient BackProp. In: Orr, G.B., Müller, K.-R. (Eds.), Neural Networks: Tricks of the Trade. Springer, pp. 9–48.
Lekson, S.H., 1988. The idea of the kiva in anasazi archaeology. KIVA 74, 203–225.
Liaw, A., Wiener, M., 2002. Classification and regression by randomForest. R. News 2, 18–22.
Lightfoot, R.R., 1994. The duckfoot site, ume 2. *Archaeology of the House and Household,* Crow Canyon Archaeological Center, Cortez.
Lipe, W.D., 1974. A conservation model for American archaeology. KIVA 39, 213–245.
Lipe, W.D., 1989. Social scale of Mesa Verde anasazi kivas. In: Lipe, W.D., Hegmon, M. (Eds.), The Architecture of Social Integration in Prehistoric Pueblos. Crow Canyon Archaeological Center, Cortez, pp. 53–71.
Lipe, W.D., 2006. Notes from the north. In: Lekson, S.H. (Ed.), The Archaeology of Chaco Canyon: an Eleventh-Century Pueblo Regional Center. School for Advanced Research Press, Santa Fe, pp. 261–314.
Lipe, W.D., Ortman, S.G., 2000. Spatial patterning in northern san juan villages, A.D. 1050–1300. KIVA 66, 91–122.
Lipe, W.D., Varien, M.D., Wilshusen, R.H. (Eds.), 1999. Colorado Prehistory: A Context for the Southern Colorado River Basin. Colorado Archaeological Society, Denver.
Mahoney, N.M., Adler, M.A., Kendrick, J.W., 2000. The changing scale and configuration of Mesa Verde communities. KIVA 66, 67–90.
Marin, A., 2010. Riders under storms: contributions of nomadic herders' observations to analysing climate change in Mongolia. Global Environ. Change 20, 162–176.
Matero, F., Fong, K.L., Bono, E.D., Goodman, M., Kopelson, E., McVey, L., Sloop, J., Turton, C., 1998. Archaeological site conservation and management: an appraisal of recent trends. Conserv. Manag. Archaeol. Sites 2, 129–142.
McIntosh, G., Catanzariti, G., 2006. An introduction to archaeomagnetic dating. Geochronometria - Journal on Methods and Applications of Absolute Chronology 25, 11–18.
Mills, B.J., 1999. Ceramics and social contexts of food consumption in the northern southwest. In: Skibo, J.M., Feinman, G.M. (Eds.), Pottery and People: A Dynamic Interaction. University of Utah Press, Salt Lake City, pp. 99–114.
Mills, B.J., Ferguson, T.J., 1998. Preservation and research of sacred sites by the zuni Indian tribe of New Mexico. Hum. Organ. 57, 30–42.
Nelson, M.C., Schachner, G., 2002. Understanding abandonments in the north American southwest. J. Archaeol. Res. 10, 167–206.
Odikwa, H.N., Ifeanyi-Reuben, N., Thom-Manuel, O.M., 2020. An improved approach for hidden nodes selection in artificial neural network. International Journal of Applied Information Systems 12, 7–14.
Oonk, S., Spijker, J., 2015. A supervised machine-learning approach towards geochemical predictive modelling in archaeology. J. Archaeol. Sci. 59, 80–88.
Orengo, H.A., Garcia, A., Conesa, F.C., Green, A., Singh, R.N., Petrie, C.A., 2019. Combining TanDEM-X with multi-temporal, multi-source satellite data for the reconstruction of the Bronze Age landscapes of the Indus Civilisation. IGARSS 2019 - 2019 IEEE International Geoscience and Remote Sensing Symposium. IEEE, Yokohama, pp. 4581–4584.
Orengo, H.A., Garcia-Molsosa, A., 2019. A brave new world for archaeological survey: automated machine learning- based potsherd detection using high-resolution drone imagery. J. Archaeol. Sci. 112, 1–12.
Ortman, S.G., Glowacki, D.M., Churchill, M.J., Kuckelman, K.A., 2000. Pattern and variation in northern san juan village histories. KIVA 66, 123–146.
Ortman, S.G., Glowacki, D.M., Varien, M.D., Johnson, C.D., 2012. The study area and the ancestral Pueblo occupation. In: Kohler, T.A., Varien, M.D. (Eds.), Emergence and Collapse of Early Villages: Models of Central Mesa Verde Archaeology. University of California Press, Berkeley, pp. 15–40.
Ortman, S.G., Varien, M.D., Gripp, T.L., 2007. Empirical bayesian methods for archaeological survey data: an application from the Mesa Verde region. Am. Antiq. 72, 241–272.
Panchal, F.S., Panchal, M., 2014. Review on Methods of Selecting Number of Hidden Nodes in Artificial Neural Network.
Peeples, M.A., Mills, B.J., Clark, J.J., Aragon, L., Giomi, E., Bellorado, B.A., 2016. Chaco Social Networks Database. Version 1.0, Southwest Social Networks Project. https://www.archaeologysouthwest.org/projects/chaco-social-networks/.
Peterson, C.E., Drennan, R.D., 2005. Communities, settlements, sites, and surveys: regional-scale Analysis of prehistoric human interaction. Am. Antiq. 70, 5–30.
Peterson, C.E., Drennan, R.D., 2011. Patterned variation in regional trajectories of community growth. In: Smith, M.E. (Ed.), The Comparative Archaeology of Complex Societies. Cambridge University Press, Cambridge, pp. 88–137.
Reese, K.M., 2018. Fieldwork Episode Report 2018: Preliminary Survey of Bureau of Land Management Sites on the Mesa Verde North Escarpment. Bureau of Land Management, Dolores.
Reese, K.M., 2019. Fieldwork Episode Report 2019: Survey of Bureau of Land Management Sites on the Mesa Verde North Escarpment. Bureau of Land Management, Dolores.
Reese, K.M., 2020. Check dam agriculture on the Mesa Verde cuesta. J. Archaeol. Sci.: Report 31, 1–10.
Reese, K.M., 2021. Mesa Verde North Escarpment Survey: Class III Survey of State-Managed Land on the Mesa Verde North Escarpment, Montezuma County, Colorado. History Colorado Center, Denver.
Reese, K.M., Glowacki, D.M., Kohler, T.A., 2019. Dynamic communities on the Mesa Verde cuesta. Am. Antiq. 84, 728–747.
Ripley, B.D., 1996. Pattern Recognition and Neural Networks. Cambridge University Press.
Roberts, R.G., Jacobs, Z., Li, B., Jankowski, N.R., Cunningham, A.C., Rosenfeld, A.B., 2015. Optical dating in archaeology: thirty years in retrospect and grand challenges for the future. J. Archaeol. Sci. 56, 41–60.
Rohn, A., 1977. Cultural Change and Continuity on Chapin Mesa. Regents Press of Kansas, Lawrence.
Rohn, A.H., Swannack Jr., J.D., 1965. Mummy lake gray: a new pottery type. Am. Antiq. 14–18.
Schachner, G., Throgmorton, K., Wilshusen, R.H., Allison, J.R., 2012. Early pueblos in the American southwest: the loss of innocence and the origins of the early southwest

village. In: Wilshusen, R.H., Schachner, G., Allison, J.R. (Eds.), Crucible of the Pueblos: the Early Pueblo Period in the Northern Southwest. Cotsen Institute of Archaeology Press, Los Angeles, pp. 1–13.
Schlanger, S.H., Wilshusen, R.H., 1993. Local abandonments and regional conditions in the North American Southwest. In: Cameron, C.M., Tomka, S.A. (Eds.), Abandonment of Settlements and Regions: Ethnoarchaeological and Archaeological Approaches. Cambridge University Press, Cambridge, pp. 85–98.
Schwindt, D.M., Bocinsky, R.K., Ortman, S.G., Glowacki, D.M., Varien, M.D., Kohler, T. A., 2016. The social consequences of climate change in the central Mesa Verde region. Am. Antiq. 81, 74–96.
Severance, O., 2015. Southeastern Utah – it's not southwestern Colorado: milk ranch point's contribution to A revised ceramic sequence for southeastern Utah. Pottery Southwest 31, 25–37.
Spielmann, K.A., Aggarwal, R.M., 2017. Household- vs. National-scale food storage: perspectives on food security from archaeology and contemporary India. In: Hegmon, M. (Ed.), The Give and Take of Sustainability: Archaeological and Anthropological Perspectives on Tradeoffs. Cambridge University Press, Cambridge, pp. 244–271.
Spielmann, K.A., Peeples, M.A., Glowacki, D.M., Dugmore, A., 2016. Early warning signals of social transformation: a case study from the US southwest. PloS One 11, e0163685.
Stathakis, D., 2009. How many hidden layers and nodes? Int. J. Rem. Sens. 30, 2133–2147.
Sullivan III, A.P., Becher, M.E., Downum, C.E., 1995. Tusayan white ware chronology: new archaeological and dendrochronological evidence. KIVA 61, 175–188.
Svetlik, I., Jull, A.J.T., Molnár, M., Povinec, P.P., Kolář, T., Demján, P., Brabcova, K.P., Brychova, V., Dreslerová, D., Rybníček, M., Simek, P., 2019. The best possible time resolution: how precise could a radiocarbon dating method Be? Radiocarbon 61, 1729–1740.
Swingler, K., 1996. Applying Neural Networks: A Practical Guide. Academic Press, London.
Toll, H.W., McKenna, P.J., 1987. The ceramography of Pueblo alto. In: Mathien, F.J., Windes, T.C. (Eds.), *Investigations At the Pueblo Alto Complex: Chaco Canyon, New Mexico, 1975–1979*, National Park Service. U.S. Department of the Interior, Santa Fe, pp. 19–230.
Tsoumakas, G., Katakis, I., 2007. Multi-label classification: an overview. Int. J. Data Warehous. Min. 3, 1–13.
U.S. Geological Survey, EROS Data Center, 1999. National Elevation Dataset. U.S. Geological Survey, Sioux Falls, South Dakota.
van Etten, J., 2017. R package gdistance: distances and routes on geographical grids. J. Stat. Software 76, 21.
Varien, M.D., 1999. Sedentism and Mobility in a Social Landscape: Mesa Verde and beyond. University of Arizona Press, Tucson.
Varien, M.D., 2010. Depopulation of the northern san juan region: historical review and archaeological context. In: Kohler, T.A., Varien, M.D., Wright, A.M. (Eds.), Leaving Mesa Verde: Peril and Change in the Thirteenth-Century Southwest. University of Arizona Press, Tucson, pp. 1–33.
Varien, M.D., Coffey, G., 2017. Community Center Reassessment Project Evaluation of Sites on Lands Administered by Bureau of Land Management. Crow Canyon Archaeological Center, Cortez, p. 2017.
Varien, M.D., Lipe, W.D., Adler, M.A., Thompson, I.M., Bradley, B.A., 1996. Southwest Colorado and southeast Utah settlement patterns, A.D. 1100–1300. In: Adler, M.A. (Ed.), The Prehistoric Pueblo World, A. D 1150–1350. University of Arizona Press, Tucson, pp. 86–113.
Varien, M.D., Ortman, S.G., 2005. Accumulations research in the southwest United States: middle range theory for big-picture problems. World Archaeol. 37, 132–155.
Varien, M.D., Ortman, S.G., Kohler, T.A., Glowacki, D.M., Johnson, C.D., 2007. Historical ecology in the Mesa Verde region: results from the village Ecodynamics project. Am. Antiq. 72, 273–299.
Varien, M.D., Wilshusen, R.H., 2002. A partnership for understanding the past: crow canyon research in the central Mesa Verde region. In: Varien, M.D., Wilshusen, R.H. (Eds.), Seeking the Center Place: Archaeology and Ancient Communities in the Mesa Verde Region. University of Utah Press, Salt Lake City, pp. 3–23.
Verdonck, L., Launaro, A., Vermeulen, F., Millett, M., 2020. Ground-penetrating radar survey at Falerii Novi: a new approach to the study of Roman cities. Antiquity 94, 705–723.
Wang, S.-C., 2003. Artificial neural network. Interdisciplinary Computing in Java Programming. Springer, pp. 81–100.
West, C.T., Roncoli, C., Ouattar, F., 2008. Local perceptions and regional climate trends on central plateau of Burkina Faso. Land Degrad. Dev. 19, 289–304.
Wilshusen, R.H., 1986. Excavations at rio vista village (site 5MT2182), a multicomponent Pueblo I village. In: Kane, A.E., Robinson, C.K. (Eds.), Dolores Archaeological Program: Anasazi Communities at Dolores: Middle Canyon Area. Bureau of Reclamation; Engineering and Research Center, Denver, pp. 210–658.
Wilshusen, R.H., 1999. Basketmaker III (A.D. 500–750). In: Lipe, W.D., Varien, M.D., Wilshusen, R.H. (Eds.), Colorado Prehistory: A Context for the Southern Colorado River Basin. Colorado Council of Professional Archaeologists, Denver, pp. 166–195.
Wilshusen, R.H., 2018. How agriculture took hold in the Mesa Verde region: a review of recent research on the late basketmaker-early Pueblo periods (AD 500–920). Reviews in Colorado Archaeology 1, 69–95.
Wilshusen, R.H., Glowacki, D.M., 2017. An archaeological history of the Mesa Verde region. In: Mills, B.J., Fowles, S.M. (Eds.), The Oxford Handbook of Southwest Archaeology. Oxford University Press, New York, pp. 307–322.
Wilshusen, R.H., Ortman, S.G., 1999. Rethinking the Pueblo I period in the san juan drainage: aggregation, migration, and cultural diversity. KIVA 64, 369–399.
Wilshusen, R.H., Perry, E.M., 2008. Evaluating the emergence of early villages in the north American southwest in light of the proposed neolithic demographic transition. In: Bocquet-Appel, J.-P., Bar-Yosef, O. (Eds.), The Neolithic Demographic Transition and its Consequences. Springer, Berlin, pp. 417–438.
Wilshusen, R.H., Schachner, G., Allison, J.R. (Eds.), 2012. Crucible of Pueblos: the Early Pueblo Period in the Northern Southwest. Cotsen Institute of Archaeology Press, Los Angeles. Monograph 71.
Wilson, C.D., 1996. Ceramic pigment distributions and regional interaction: a Re-examination of interpretations in shepard's "technology of La plata pottery". KIVA 62, 83–102.
Wilson, D.C., Blinman, E., 1995. Ceramic types of the Mesa Verde region. In: R H B, Bradley Jr., B., Chandler, S.M. (Eds.), Archaeological Pottery of Colorado: Ceramic Clues to the Prehistoric and Protohistoric Lives of the State's Native Peoples. Colorado Council of Professional Archaeologists, pp. 33–88.
Żabiński, G., Gramacki, J., Gramacki, A., Mišta-Jakubowska, E., Birch, T., Disser, A., 2020. Multi-classifier majority voting analyses in provenance studies on iron artefacts. J. Archaeol. Sci. 113, 105055.